Anal Bioanal Chem (2013) 405:3773–3781
DOI 10.1007/s00216-012-6491-8

ORIGINAL PAPER

Supramolecular immobilization of glucose oxidase on gold coated with cyclodextrin-modified cysteamine core PAMAM G-4 dendron/Pt nanoparticles for mediatorless biosensor design

Paula Díez · Ciprian-George Piuleac · Paloma Martínez-Ruiz · Santiago Romano · María Gamella · Reynaldo Villalonga · José M. Pingarrón

Received: 9 August 2012 / Revised: 28 September 2012 / Accepted: 9 October 2012 / Published online: 23 October 2012

Abstract Cysteamine core polyamidoamine G-4 dendron branched with β-cyclodextrins was chemisorbed on the surface of Au electrodes and further coated with Pt nanoparticles. Adamantane-modified glucose oxidase was subsequently immobilized on the nanostructured electrode surface by supramolecular association. This enzyme electrode was used to construct a reagentless amperometric biosensor for glucose, making use of the electrochemical oxidation of H_2O_2 generated in the enzyme reaction. The amperometric response of the biosensor was rapid (6 s) and a linear function of glucose concentration between 5 and 705 $\mu mol L^{-1}$. The biosensor had a low detection limit of 2.0 $\mu mol L^{-1}$, sensitivity of 197 $mA mol^{-1} L cm^{-2}$, and retained 94 % of its initial response after storage for nine days at 4 °C.

Published in the topical collection in *Bioelectroanalysis* with guest editors Nicolas Plumeré, Magdalena Gebala, and Wolfgang Schuhmann.

Electronic supplementary material The online version of this article (doi:10.1007/s00216-012-6491-8) contains supplementary material, which is available to authorized users.

P. Díez · M. Gamella · R. Villalonga (✉) · J. M. Pingarrón (✉)
Department of Analytical Chemistry, Faculty of Chemistry,
Complutense University of Madrid,
28040 Madrid, Spain
e-mail: rvillalonga@quim.ucm.es
e-mail: pingarro@quim.ucm.es

C.-G. Piuleac
Department of Chemical Engineering,
"Gh. Asachi" Technical University,
Bd. D. Mangeron No. 71A,
700050 Iasi, Romania

P. Martínez-Ruiz · S. Romano
Department of Organic Chemistry I, Faculty of Chemistry,
Complutense University of Madrid,
28040 Madrid, Spain

Keywords Biosensor · β-cyclodextrin · Dendrimer · Glucose oxidase · Platinum nanoparticles · Supramolecular complex

Introduction

The development of enzyme-based electrochemical biosensors has received much attention because of their potential use as highly selective analytical devices in chemical and clinical laboratories, the food industry, environmental monitoring, and other, related, fields [1]. In general, the development and performance of enzyme biosensors are directly linked to the strategy used to immobilize the protein on the transducer surface, and to the physicochemical properties of the materials used to design the electrodes [2].

Biosensor technology has been promoted by the use of nanosized materials in the design of electrodes with novel structures [3]. Hard nanomaterials, for example metal and metal oxide nanoparticles [4, 5], graphene [6], and carbon nanotubes [7], have been widely used to create reliable biosensor surfaces. These developments have been supported by the unique properties of these nanomaterials, for example high surface energy and surface-to-volume ratio, the ability to reduce the protein–metal particle distance, high electroconductivity and protein load capacity, the ability to catalyze the electrochemical processes associated with several compounds produced in enzyme-mediated reactions, and the possibility of acting as electroconductive wires between the enzyme and the electrode substrate [2].

Organic polymer-based nanomaterials, for example dendrimers and dendrons, have been also used in biosensor design [8, 9]. These soft nanomaterials are monodisperse macromolecules with a regular and highly branched three-

dimensional structure. They have a high structural homogeneity, surface reactivity, and molecular host capacity [10], which are important characteristics for multipoint immobilization of enzymes on electrode surfaces. In addition, it has been demonstrated that metal nanoparticles can be stabilized in aqueous media by polyamidoamide (PAMAM) dendritic structures—by interaction with primary amino groups on the polymer surface and by association with amide and tertiary amine groups in the cavities of the dendrimer [11, 12]. These properties can be used to prepare stable hybrid nanomaterials based on metal nanoparticles–PAMAM dendritic structures for suitable modification of electrode surfaces and further construction of electrochemical enzyme biosensors [13, 14].

Functionalization of solid surfaces with enzymes and other proteins is of crucial importance not only in biosensor technology but has also in the future development of advanced biomaterials, biotechnological processes, and biologically inspired nanomaterials. Generally, proteins can be immobilized on solid surfaces by covalent bonding, physical entrapment and/or encapsulation, and adsorption. Although covalent attachment and physical entrapment and/or encapsulation result in greater stability, enzyme activity is often reduced by harsh reaction conditions and the large distance between substrates and enzymes. Enzymes are easily immobilized under mild conditions by use of adsorption strategies, but the stability of such adducts is low and the proteins can often be easily released from the supports. An alternative approach to immobilization of enzymes on solid supports is the formation of multipoint supramolecular complexes based on the complementary host–guest properties of β-cyclodextrin (CD) and 1-adamantane derivatives [15]. Such supramolecular strategies have previously been used for successful construction of amperometric enzyme biosensors [16–18].

In this work, modification of gold surfaces with CD-modified PAMAM dendron/Pt nanoparticles (PtNPs) was followed by supramolecular immobilization of adamantane-modified glucose oxidase (GO, EC 1.1.3.4) on the hybrid nanomaterial. The rationale for this original approach is based on the use of a thiol-containing CD-modified PAMAM dendron derivative as a permeable and stable coating material for the electrode surface. This hyperbranched polymer has molecular receptor capacity because of branched CD moieties favoring the formation of host–guest supramolecular complexes with adamantane-modified enzymes. The PAMAM dendron derivative also has the capacity to stabilize PtNPs, enabling the preparation of an inorganic–organic hybrid nanomaterial able to catalyze the transformation of H_2O_2, thus enabling construction of a third-generation GO-based biosensor for glucose. GO was selected as model enzyme because of its importance in biosensor technology for glucose detection [19] and because extensive studies have been conducted on GO-based amperometric biosensors, thus enabling reliable comparison of the performance of the new biosensor, designed by use of a hybrid nanomaterial and supramolecular enzyme immobilization.

Materials and methods

Reagents and apparatus

Glucose oxidase, cystamine core PAMAM G-4 dendrimer, and CD were purchased from Sigma–Aldrich (USA). Other chemicals were analytical grade or higher.

Amperometric measurements were performed with a dual-channel ultrasensitive Inbea amperometric detector (Inbea Biosensores, Spain). The cyclic voltammetry (CV) and the electrochemical impedance spectroscopy (EIS) experiments were performed with a FRA2 μAutolab Type III potentiostat/galvanostat. Data were acquired by use of GPES ver. 4.9 and Frequency Response Analyser software (Metrohm Autolab, The Netherlands). A conventional three-electrode system was used in all electrochemical studies. A gold disk (CHI Instruments, UK; 2.0 mm diameter) modified with the CD-PAMAM dendron–PtNPs hybrid nanomaterial and the enzyme was regarded as the working electrode. An Ag/AgCl/KCl (3 $mol L^{-1}$) electrode and a Pt wire were used as reference and counter electrodes, respectively. All the measurements with the modified electrode were carried out at 25 °C in 0.1 $mol L^{-1}$ sodium phosphate buffer at pH 7.0 (working volume 10 mL). Amperometric measurements were accomplished in stirred solutions at 300 rpm. Glucose solutions (5.0 $mmol L^{-1}$) in 50 $mmol L^{-1}$ sodium phosphate buffer, pH 7.0, were freshly prepared.

Transmission electron microscopy (TEM) measurements were performed with a Jeol (Japan) JEM-2100 microscope. The surface of the nanostructured electrode was investigated by high-resolution field-emission scanning electron microscopy (SEM) with a Jeol JSM-6335 F instrument. The morphology of the gold-modified surface was studied by atomic-force microscopy (AFM) with an SPM Nanoscope IIIa multimode microscope (Veeco Instruments, USA). Surface plasmon resonance (SPR) measurements were performed at a fixed wavelength of 670 nm by means of a Springle Autolab-SPR equipment from Metrohm Autolab. ^1H NMR characterization was performed with a Bruker Avance 500-MHz spectrometer (Bruker BioSpin, Germany).

Synthesis of CD-modified cysteamine core PAMAM G-4 dendron (CD-PAMAM G-4)

Fifty milligrams of cystamine core PAMAM G-4 dendrimer and 510 mg mono-6-*O*-tosyl CD (CDTs) were dissolved in 100 mL deoxygenated DMSO and the mixture was stirred at room temperature under an N_2 atmosphere for four days. The solution was then concentrated under vacuum to 5 mL, diluted

with 150 mL distilled water and, finally, dialyzed against distilled water by use of Amicon Ultra-15 centrifugal filter units with Ultracel-10 membranes (Millipore, USA). Subsequently, the solution was concentrated to 20 mL and treated with $NaBH_4$ solution (10 mmolL^{-1} final concentration) for 2 h with magnetic stirring. The mixture was then dialyzed and concentrated by use of Amicon centrifugal filter units as described above, yielding a CD-PAMAM G-4 solution of 4 mgmL^{-1} final concentration (yield 93 mg). The CD-PAMAM G-4 dendron was characterized by ^{1}H NMR in D_2O.

Preparation of the GO-ADA/CD-PAMAM/PtNP/Au enzyme electrode

First, GO was modified with 1-adamantanecarboxylic acid (GO-ADA), as described elsewhere [16], then concentrated by use of Amicon centrifugal filter units to a final concentration of 5 mgmL^{-1} in 50 mmolL^{-1} sodium phosphate buffer, pH 7.0. A gold disk electrode was polished with alumina powder (0.3 μm) then rinsed with double-distilled water and immersed in an ultrasonic bath for 5 min. The electrode was then dipped in boiling 8 molL^{-1} KOH solution for 1 h, washed with distilled water, and immersed in piranha solution for 30 min. It was then electrochemically treated by cyclic voltammetry in 0.1 molL^{-1} H_2SO_4 solution through twenty cycles between −0.2 V and 1.85 V at a scan rate of 100 mVs^{-1}. The cleaned gold surface was first dipped into 10 mL 0.5 mgmL^{-1} CD-PAMAM G-4 aqueous solution to coat the metal surface with a CD-branched dendron derivative monolayer. After incubation for 2 h, the modified electrode was washed several times with distilled water and subsequently dipped into 10 mL 10 mmol L^{-1} H_4PtCl_6 solution. After incubation for 10 min with continuous magnetic stirring, 1.0 mL 50 mmolL^{-1} $NaBH_4$ solution was added to cause PtNPs formation. The electrode was kept in the stirred solution for 10 min, then exhaustively washed with distilled water and finally coated with 20 μL 5 mgmL^{-1} GO-ADA solution. Immobilization of the enzyme was accomplished by allowing the incubation to proceed for 2 h at 4 °C. Finally, the enzyme electrode was washed with cold 50 mmolL^{-1} sodium phosphate buffer solution, pH 7.0, and kept at 4 °C in this solution until use.

Results and discussion

Preparation and characterization of the enzyme electrode

The strategy used to prepare the Au electrode surface functionalized with the CD-branched PAMAM G-4 dendron–PtNPs hybrid nanomaterial and its further use as support for the supramolecular immobilization of GO-ADA is illustrated schematically in Fig. 1.

First, cystamine core PAMAM G-4 dendrimer was reacted with mono-6-*O*-tosyl-βCD to introduce molecular receptor functionality at the dendrimer surface, using the primary amino groups of the dendrimer shell as the branching point. The CD-modified cystamine core PAMAM G-4 dendrimer was then reduced with $NaBH_4$ to cleave the disulfide bond at the dendrimer core. The resulting water-soluble CD-branched cysteamine core PAMAM G-4 dendron contained an active thiol group which could be chemisorbed on the gold electrode surface.

This hyperbranched polymer derivative was characterized by ^{1}H NMR (Fig. S1 in the Electronic Supplementary Material). It was observed that nine CD units were attached to each PAMAM G-4 dendron molecule, because of modification of 28 % of the primary amino groups in the polymer. This partial modification could be explained on the basis of the steric hindrance caused by the bulky CD moieties attached to the dendron surface. This prevented further reaction of other mono-6-*O*-tosyl-βCD molecules with the remaining amino groups of the modified dendritic molecule.

The capability of this dendron derivative to act as a host receptor for the supramolecular recognition of adamantane-modified GO was evaluated by SPR measurements. Figure 2 shows the changes produced in the SPR signal of the gold surface after sequential exposure to different cysteamine core PAMAM G-4 dendron and GO derivatives. Incubation with the two different cysteamine core PAMAM G-4 dendron derivatives (with and without CD attached) produced a similar and noticeable increase in the SPR signal which was barely affected by washing. This result suggested the thiol-containing dendron derivatives were successfully chemisorbed on the Au surface and the process was not significantly affected by the presence of the branching CD moieties at the surface of the dendritic structure.

Further, incubation of the Au surface coated with the CD-modified dendron in the adamantane-modified GO solution at pH 7.0 caused a further significant increase in the SPR signal (sensogram a), thus demonstrating the interaction between the functionalized enzyme molecules and the surface capped with the CD-modified dendron. On the basis of on the presence of bulky CD groups on the dendron surface, the contribution of host–guest supramolecular association to the whole interaction observed by SPR could be predicted. However, a similar increase in the SPR signal was observed for the Au surface coated with the cysteamine core PAMAM G-4 dendron after incubation with native GO (curve b). It has been reported that the primary and tertiary amino groups located on the surface and in the cavity of PAMAM G-4 dendrimers have pK_a values of 9.0 and 5.8, respectively [20]. Thus, at pH 7.0, PAMAM G-4 dendrimers can bear a positive charge by protonation of the primary amines at the rim. Moreover, the isoelectric point of native GO is 4.2 and, consequently, it is negatively charged at pH 7.0. As a consequence, GO is readily immobilized on the

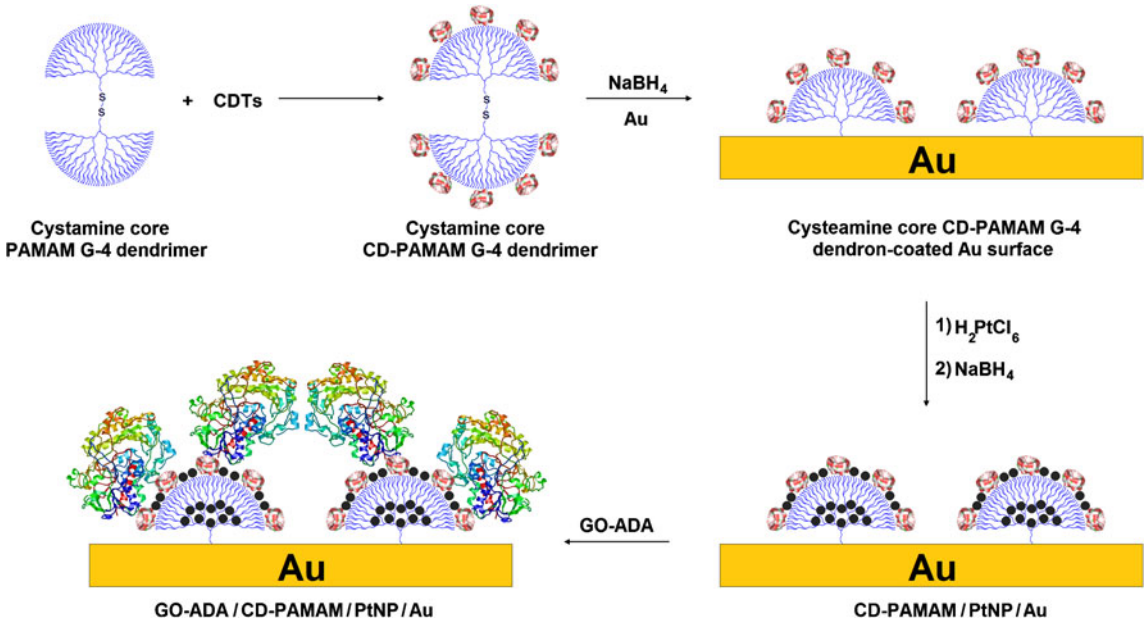

Fig. 1 Schematic diagram of the steps involved in preparation of GO-ADA/CD-PAMAM/PtNP/Au based enzyme biosensors

PAMAM G-4 dendron-coated Au surface by polyelectrostatic interactions.

Loading of native GO on the Au surface coated with the CD-modified dendron was less favored, according to the low increase observed in the SPR signal (curve c). The result led to modification of the primary amino groups with the bulky oligosaccharide moieties at the surface of the dendron, reducing the positive electrostatic field around this polymer. It also caused noticeable steric hindrance which reduced interaction of the dendron with the GO molecules.

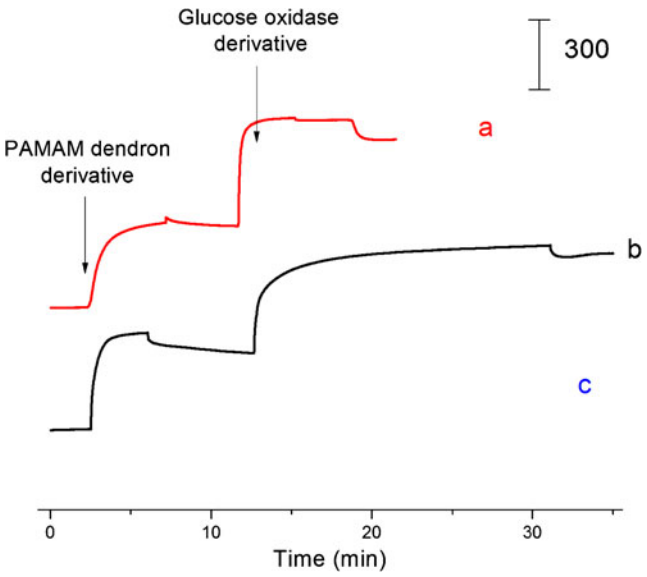

Fig. 2 SPR sensogram recorded on Au surfaces upon successive incubation with CD-PAMAM G-4 and GO-ADA (**a**), PAMAM G-4 and GO (**b**) and CD-PAMAM G-4 and GO (**c**)

The CD-PAMAM G-4-coated gold surface was coated with Pt nanoparticles. The procedure described in the "Materials and methods" section produced small and spherically-shaped Pt nanoparticles with an average size of 2.6±0.4 nm, as revealed by TEM. As can be shown by SEM analysis (Fig. 3), the dendron-modified gold surface was coated with a stable three-dimensional arrangement of Pt nanoparticles in which the protuberant nanostructures are combined with deep nanoholes. The high density of Pt nanoparticles prevented characterization of this surface by SPR measurements.

This modified Au surface was further used as support for immobilization of the adamantane-modified GO derivative. The changes on the topology and the electrochemical characteristics of the Au surface after the different modification steps were checked by AFM, EIS, and CV.

The tapping mode AFM images for different gold surfaces are presented in Fig. 4. Characteristic flat topology was observed for the unmodified gold surface; average roughness was 0.9 nm and average height was 3.2 nm (maximum 5.6 nm).

Coating with the CD-PAMAM dendron derivative yielded a modified surface pattern with ellipsoidal nanostructures; average roughness was 3.1 nm and average height 12.0 nm (maximum 18.6 nm). After deposition of Pt nanoparticles on the dendron-modified surface, a more irregular pattern was observed with a higher density of protuberant nanostructures; average and maximum height were 34.6 nm and 92.9 nm, respectively, and average roughness of 15.1 nm was estimated for the Pt nanoparticles-modified surface.

This surface was softened after immobilization of the enzyme derivative. In fact, the average roughness and height, respectively, decreased to approximately 10.3 nm and 19.2 nm after incubation in the GO-ADA solution. The maximum

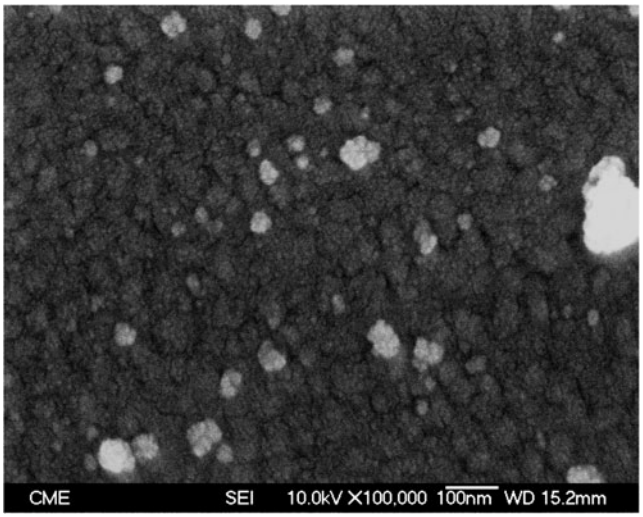

Fig. 3 Field-emission SEM image of the CD-PAMAM G-4/PtNP-modified Au surface

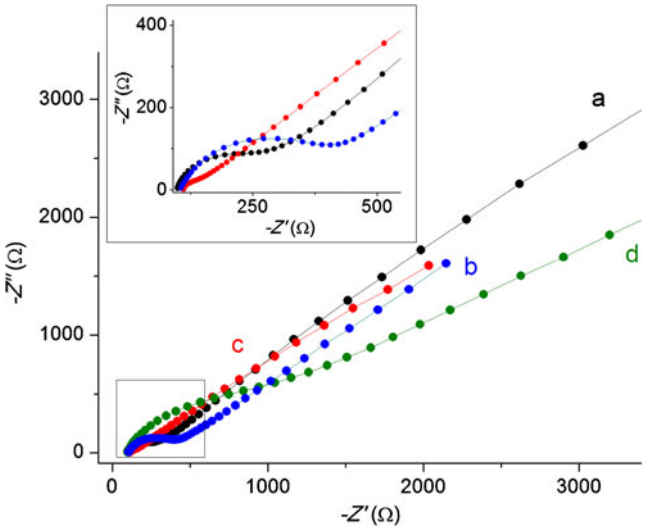

Fig. 5 Nyquist plots of bare Au (**a**), CD-PAMAM/Au (**b**), CD-PAMAM/PtNPs/Au (**c**), and GO-ADA/CD-PAMAM/PtNP/Au (**d**) electrodes in 0.1 molL^{-1} KCl solution containing 5 mmolL^{-1} $K_3[Fe(CN)_6]$–$K_4[Fe(CN)_6]$ (1:1)

height for the enzyme-coated surface was also reduced, to approximately 61.7 nm. These results suggested the enzyme molecules were homogeneously distributed over the entire PtNP-coated surface, filling the nanoholes created by these nanomaterials.

The effect of the different modification steps on the barrier properties of the gold surface was evaluated by electrochemical impedance spectroscopy in 0.1 molL^{-1} KCl solution containing 5 mmolL^{-1} $[Fe(CN)_6]^{4-/3-}$. Fig. 5 shows the resulting Nyquist plots, with R_{et}=118 Ω for the bare gold surface and a slope of 0.89 for the straight line observed over the broad range of low frequencies. This was indicative of rapid electron transfer for the $[Fe(CN)_6]^{4-}$ and $[Fe(CN)_6]^{3-}$ ions on the electrode surface. A small increase in the electron transfer resistance, R_{et}=195 Ω, and linear behavior at low frequencies with similar slope were observed for the electrode surface coated with the CD-modified dendron derivative. This was indicative of a low barrier effect of the dendron molecules on the electron transfer process at the electrode surface, most likely because of the permeable and polycationic nature of the polyamidoamine polymer. Also, the Nyquist plots revealed the electron-transfer resistance was reduced (R_{et}=29 Ω) after modification with the highly conductive Pt nanoparticles. However, as was expected, an opposite effect was evident

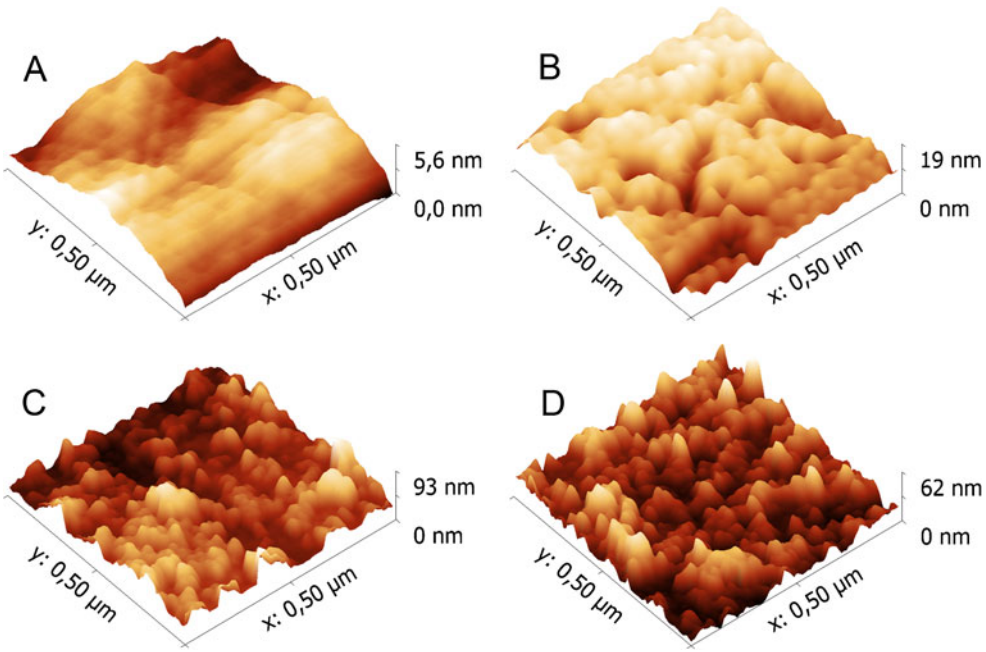

Fig. 4 Three-dimensional AFM analysis of the Au surface before (**A**) and after modification with CD-PAMAM (**B**), CD-PAMAM/PtNP (**C**) and GO-ADA/CD-PAMAM/PtNP (**D**)

after immobilization of adamantane-modified GO, which resulted in a noticeable increase in the diameter of the semicircle at high frequency (R_{et}=639 Ω). In addition, the slope of the straight line at low frequencies also decreased to 0.58. This higher resistance to electron transfer and diffusion-controlled processes suggested high coverage of the electrode surface by the non-conductive enzyme molecules.

The EIS results were confirmed by cyclic voltammetry for the different electrode structures in 5 mmolL^{-1} $[Fe(CN)_6]^{4-/3-}$ +0.1 molL^{-1} KCl solution. As can be observed in Fig. 6, the unmodified gold electrode had well-defined typical quasi-reversible diffusion-limited patterns with ΔE=99 mV and i_a/i_c=1.07. The electrochemical surface area of the bare electrode was calculated, by use of the Randles–Sevcik equation, to be 3.6 mm^2. Coating with CD-PAMAM dendron derivative caused a small decrease in both the anodic and cathodic peaks, reducing the value calculated for the electrochemical surface area to approximately 3.4 mm^2. In addition, the ΔE and i_a/i_c values were increased to 129 mV and 1.23, respectively.

A more reversible diffusion-limited pattern was observed for the electrode after modification with Pt nanoparticles, with larger anodic and cathodic peaks current values, ΔE=96 mV and i_a/i_c=1.10. Also, the metal nanoparticles slightly increased the electrochemical surface area of the electrode to 3.7 mm^2. This voltammetric behavior is attributable to the presence of the highly electroconducting Pt nanoparticles. The subsequent immobilization of the enzyme derivative on the electrode surface provoked a drastic decrease in the anodic and cathodic peak current and in the electrochemical surface area (1.74 mm^2). The enzyme loading also affected the quasi-reversible behavior of the $[Fe(CN)_6]^{4-/3-}$ electrochemical reaction at the electrode surface, with ΔE=358 mV and i_a/i_c=1.26. These results again suggested high coverage of the electrode surface by the non-conductive and bulky enzyme molecules.

Figure 7 shows the cyclic voltammograms recorded at the enzyme-modified electrode in aerated 0.1 molL^{-1} sodium phosphate buffer solution, pH 7.0, at a scan rate of 50 mV s^{-1}, before and after addition of glucose. The peak observed in the absence of glucose was because of the dissolved oxygen in solution. Addition of glucose caused the appearance of anodic and cathodic peaks suggesting that the H_2O_2 formed in the enzyme reaction can be electrocatalytically oxidized and reduced at the Pt nanoparticles-modified electrode surface.

It has recently been proposed that H_2O_2 can be electrochemically transformed at the Pt surface by the following mechanisms [21]. For reduction, H_2O_2 is first dissociated to adsorbed OH on two oxide-free Pt sites in a non-electrochemical step. Because adsorbed OH on Pt is not stable at low potentials, the surface sites are rapidly regenerated in an electrochemical reduction step, leaving free the Pt sites to dissociate other H_2O_2 molecules.

$$2Pt + H_2O_2 \rightarrow 2Pt(OH)$$
$$2Pt(OH) + 2H^+ + 2e^- \rightarrow 2Pt(H_2O)$$

For oxidation at sufficiently positive potentials, at which oxygenated species are adsorbed on Pt sites, H_2O_2 is first oxidized on two OH-covered Pt sites to O_2 in a non-electrochemical step. Because the oxide-free Pt surface is not stable at high positive potentials, the reduced surface sites are then electrochemically re-oxidized and become available again to oxidize H_2O_2.

$$2Pt(OH) + H_2O_2 \rightarrow 2Pt(H_2O) + O_2$$
$$2Pt(H_2O) \rightarrow 2Pt(OH) + 2H^+ + 2e^-$$

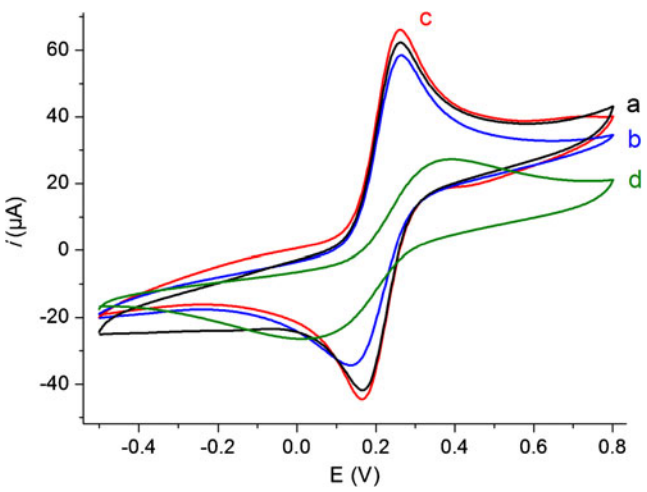

Fig. 6 Cyclic voltammograms recorded in 0.1 molL^{-1} KCl solution containing 5 mmolL^{-1} $K_3[Fe(CN)_6]$–$K_4[Fe(CN)_6]$ (1:1) at bare Au (**a**), CD-PAMAM/Au (**b**), CD-PAMAM/PtNPs/Au (**c**), and GO-ADA/CD-PAMAM/PtNP/Au (**d**) electrodes. Scan rate 50 mV s^{-1}

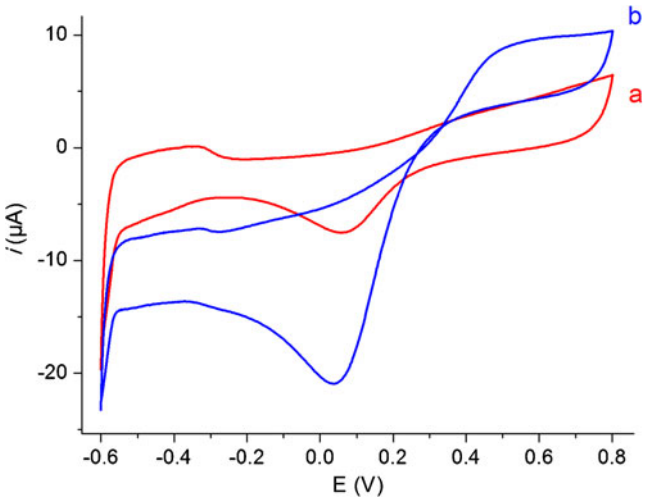

Fig. 7 Cyclic voltammograms recorded in 0.1 molL^{-1} sodium phosphate buffer, pH 7.0, at a scan rate of 50 mV s^{-1}, for a GO-ADA/CD-PAMAM/PtNP/Au electrode before (**a**) and after (**b**) addition of 200 μmolL^{-1} glucose

According to the cyclic voltammetric behavior at the GO bioelectrode, it can be concluded that H_2O_2 can be electrocatalytically oxidized at potentials higher than +340 mV. Electrocatalytic reduction of H_2O_2 can also be observed at potentials below +230 mV. These findings suggested that it was feasible to design a mediatorless electrochemical biosensor for glucose, able to work at low potentials, by using the proposed electrode surface.

The GO-ADA/CD-PAMAM/PtNP/Au electrode was further evaluated for amperometric quantification of glucose. For this purpose, the optimum working conditions were first evaluated and selected. Maximum amperometric response toward glucose was achieved in buffer solutions of pH 6.0–7.0. In addition, currents with poor signal-to-noise ratios were obtained when the potential was below +200 mV. The best results were achieved by detecting the electrochemical oxidation of the enzymatically-produced H_2O_2 at potentials higher than +350 mV. To minimize the undesirable effect of common interfering substances during amperometric detection of glucose, the lowest anodic potential at which good signal-to-noise ratios were observed was selected. Summarizing, further amperometric measurements were performed in 0.1 molL^{-1} sodium phosphate buffer of pH 7.0 at a constant potential of +400 mV vs Ag/AgCl.

Under these conditions, the dynamic amperometric response of the bioelectrode upon successive addition of 5.0 mmolL^{-1} glucose is illustrated in Fig. 8 (curve a). For control measurements, Au electrodes coated with PAMAM/PtNP (curve b), CD-PAMAM/PtNP (curve c), PtNP (curve d) and PAMAM (data not shown), on which equivalent activity of native GO was immobilized under similar conditions, were also checked. The GO-ADA/CD-PAMAM/PtNP/Au-based biosensor had a rapid catalytic response, reaching 95 % of the steady-state current in approximately 6 s. No significant increase in the anodic current was observed for the GO/PAMAM/Au electrode, demonstrating that PtNPs are needed for electrocatalytic oxidation of H_2O_2 at +400 mV. The amperometric responses of the control electrodes were significantly lower, suggesting greater amount of immobilized active enzyme on the GO-ADA/CD-PAMAM/PtNP/Au electrode, probably as a result of host–guest and electrostatic interactions.

Biosensor response was a linear function of glucose concentration in the range 5 to 705 μmolL^{-1}; the equation of the plot was i_a (mA)=7.1×c (glucose; molL^{-1})+7×10^{-5} (n=10, r=0.999). A similar range of linear response was observed for the control GO/PAMAM/PtNP/Au electrode. However, a shorter range (5–470 μmolL^{-1}) was observed for the GO/CD-PAMAM/PtNP/Au biosensor. The equations describing the linear response of these control biosensors were:

$$i_a(\mathrm{mA}) = 2.4 \times c(\text{glucose; mol L}^{-1}) + 1 \times 10^{-5} \quad (\mathrm{GO/PAMAM/PtNP/Au})$$
$$i_a(\mathrm{mA}) = 1.3 \times c(\text{glucose; mol L}^{-1}) + 6 \times 10^{-6} \quad (\mathrm{GO/CD-PAMAM/PtNP/Au})$$

The sensitivity of the GO-ADA/CD-PAMAM/PtNP/Au biosensor was determined to be 197 mA mol^{-1} L cm^{-2}, on the basis of the electroactive area of the gold electrode. Remarkably lower sensitivity was obtained with the control enzyme electrodes—66.7 mA mol^{-1} L cm^{-2} and 36.1 mA mol^{-1} L cm^{-2} for GO/PAMAM/PtNP/Au and GO/CD-PAMAM/PtNP/Au, respectively. This result has indicated, again, lower enzyme loading on the control biosensors. This suggests that enzyme immobilization on the different Pt nanoparticle-modified surfaces followed behavior similar to that that deduced from the SPR experiments.

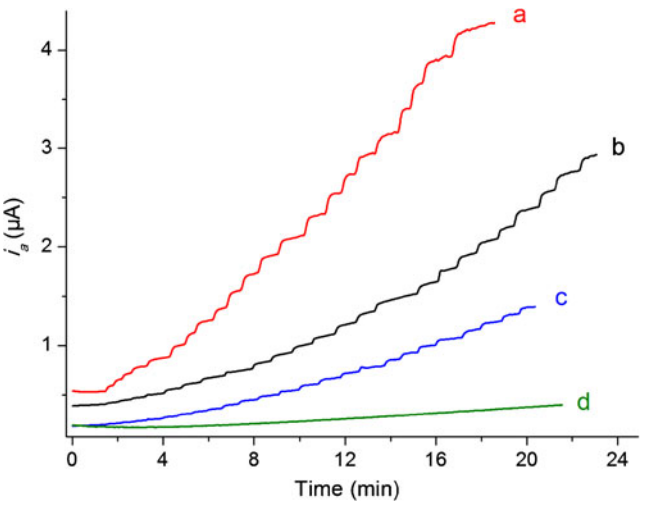

Fig. 8 Amperometric responses recorded with GO-ADA/CD-PAMAM/PtNP/Au (**a**), GO/PAMAM/PtNP/Au (**b**), GO/CD-PAMAM/PtNP/Au (**c**), and GO/PtNP/Au (**d**) electrodes on successive additions of 5.0 mmolL^{-1} glucose. E_{app}=+ 400 mV

For the GO-ADA/CD-PAMAM/PtNP/Au biosensor the detection limit for glucose was 2.0 μmolL^{-1}, calculated in accordance with the $3S_b/m$ criterion, where m was the slope of the linear calibration plot and S_b was estimated as the standard deviation (n=10) of signals corresponding to the lowest glucose concentration which could be quantitatively measured with the biosensor. In addition, the apparent Michaelis–Menten constant of the biosensor for glucose was estimated as K_M^{ap}=500 μmolL^{-1}, which was much lower than that previously reported for *Aspergillus niger* glucose oxidase at pH 5.6 (K_M=33 mmolL^{-1}) [22], indicating that the affinity of the substrate for the enzyme was not worsened by using supramolecular immobilization and the developed electrode structure.

In Table 1 the analytical characteristics of the GO-ADA/CD-PAMAM/PtNP/Au biosensor are compared with those reported recently for other mediatorless glucose oxidase biosensors. It is apparent the detection limit, sensitivity, and apparent Michaelis–Menten constant are among the best reported. They are only surpassed by biosensors using extreme working potentials and which are, as a result, more susceptible to interference by other analytes during glucose determination.

The good electroanalytical behavior of the GO-ADA/CD-PAMAM/PtNP/Au biosensor could be assigned to the large amount of immobilized enzyme, and the cooperative contribution of several factors to maintaining the active enzyme protein conformation on the electrode surface. In particular, the supramolecular strategy used for GO immobilization and the presence of metal nanoparticles should eliminate structural deformation of the active globular enzyme on immobilization on the electrode surface. In addition, the presence of highly hydrophilic CD-PAMAM G-4 dendron units on that surface should contribute to keeping a hydrophilic microenvironment around the enzyme. The occurrence of randomly arranged nanocavities on the Pt nanoparticles should also ensure a high loading of immobilized enzyme in these nanoholes. It is also expected that such nanostructures should protect the hydrophilic microenvironment around the immobilized enzyme.

Measurement of the repeatability of measurement of 25 $\mu mol L^{-1}$ glucose with one GO-ADA/CD-PAMAM/PtNP/Au electrode ($n=10$) yielded a relative standard deviation (RSD) of 4.7 %. Electrode-to-electrode reproducibility was calculated from the responses obtained with ten different GO-ADA/CD-PAMAM/PtNP/Au electrodes prepared in the same manner for the same glucose concentration; the RSD was 7.2 %.

The selectivity of the enzyme electrode was evaluated by measuring the amperometric response for 25 $\mu mol L^{-1}$ glucose in the presence of seven possible interfering substances. Fructose, galactose, sucrose, arabinose, cysteine, citric acid, and caffeine at 100 $\mu mol L^{-1}$ did not cause significant changes in the steady-state current signal obtained for glucose. However, as expected, the amperometric response of the biosensor toward glucose was affected by 2.1 % and 20 % after addition of uric acid and ascorbic acid, respectively, at 2.5 $\mu mol L^{-1}$.

Regarding the effect of biosensor storage time at 4 °C under dry conditions on its amperometric response, it was observed that the biosensor retained more than 94 % of its initial activity after storage for 9 days. Longer storage times resulted in gradual loss of biosensor activity; approximately 45 % of the initial amperometric response was retained after one month. It should be also noted that the activity of the biosensor was reduced to approximately 35 % by incubation for 2 h in a saturated solution of 1-adamantane carboxylic acid; this was indicative of disruption of the supramolecular host–guest interactions between the modified enzyme molecules and the CD-branched dendron derivatives at the electrode surface.

Table 1 Comparison of the analytical performance of the GO-ADA/CD-PAMAM/PtNP/Au biosensor with that reported previously for mediatorless glucose biosensors

Electrode	E (mV)	Linear range ($\mu mol L^{-1}$)	D.L. ($\mu mol L^{-1}$)	Sensitivity ($mA mol^{-1} L cm^{-2}$)	K_M ($mmol L^{-1}$)	Ref.
Naf/GO/MWNT/Al_2O_3@SiO_2/GCE	−488[a]	17.5–800	17.5	127.0	0.5	[23]
GO/B-MWNT/GCE	−490[b]	50–300	10.0	111.6	0.2	[24]
Naf/GO/Ag-Pdop@MWNT/GCE	−496[b]	50–1100	17.0	43.8	4.56	[25]
GO/AuNPs/MWNT/PVA/GCE	−400[b]	500–8000	200	16.6	–	[26]
$[GO/PDDA]_3$/$[SDS\text{-}MWNT/PDDA]_3$/MPS/Au/Ti/PET	+600[a]	20–2200	10	5.6	5.15	[27]
GO/AuNPs/DMF/$BMIMPF_6$/GCE	−800[b]	0.1–10^3	0.1	595	0.0035	[28]
GO/PPyAA/AuNPs/GCE	+600[a]	50–1.6×10^4	50	14	1.83	[29]
Naf/GO/NP-Au	−200[b]	10–2.2×10^4	10	–	–	[30]
GO/PtNPs/MWNT/GCE	+700[a]	0.25–10^4	0.25	431	–	[31]
GO/Au/GCE	−550[b]	2.5–157.5	0.32	–	0.016	[32]
GO/PMB@SiO_2/GCE	−430[b]	10–1110	3.0	–	0.5	[33]
GO-ADA/CD-PAMAM/PtNPs/Au	+400[a]	5–705	2.0	197	0.5	This work

[a] Ag/AgCl

[b] Saturated calomel electrode

D.L., detection limit; Naf, Nafion; MWNT, multi-walled carbon nanotubes; CGE, glassy carbon electrode; B-MWNT, boron-doped MWNT; Pdop, polydopamine; NPs, nanoparticles; PVA, poly(vinyl alcohol); PDDA, polydiallyldimethylammonium chloride; SDS, sodium dodecylsulfate; MPS, 3-mercapto-1-propanesulfonic acid; PET, poly(ethylene terephthalate); $BMIMPF_6$, 1-butyl-3-methylimidazolium hexafluorophosphate; PPyAA, poly(pyrrole propylic acid); NP-Au, nanoporous Au; PMB, poly(methylene blue)

Conclusions

A novel electrode surface involving gold coated with a PtNPs-coated CD-branched cysteamine core PAMAM G-4 dendron was used as support for immobilization of adamantane-modified glucose oxidase, mainly by formation of host–guest supramolecular associations. The enzyme electrode was evaluated for construction of a third-generation biosensor for glucose. The biosensor was highly selective, with good sensitivity and stability, a low detection limit, and a rapid electroanalytical response to glucose. These results suggest the Au surface modified with this inorganic–organic hybrid nanomaterial is a useful basic electrode for preparing mediatorless, oxidase-based, amperometric enzyme biosensors.

Acknowledgements R. Villalonga acknowledges the Ramón and Cajal contract from the Spanish Ministry of Science and Innovation. Financial support from the Spanish Ministry of Science and Innovation (CTQ2011-24355, CTQ2009-12650, CTQ2009-09351) and Comunidad de Madrid S2009/PPQ-1642, programme AVANSENS, are gratefully acknowledged.

References

1. Newman JD, Setford SJ (2006) Enzymatic biosensors. Mol Biotechnol 32:249–268
2. North SH, Lock EH, Taitt CR, Walton SG (2010) Critical aspects of biointerface design and their impact on biosensor development. Anal Bioanal Chem 397:925–933
3. Li H, Liu S, Dai Z, Bao J, Yang X (2009) Applications of nanomaterials in electrochemical enzyme biosensors. Sensors 9:8547–856
4. Guo S, Dong S (2009) Biomolecule-nanoparticle hybrids for electrochemical biosensors. Trends Anal Chem 28:96–109
5. Pingarrón JM, Yáñez-Sedeño P, González-Cortés A (2008) Gold nanoparticle-based electrochemical biosensors. Electrochim Acta 53:5848–5866
6. Shao Y, Wang J, Wu H, Liu J, Aksay IA, Lin Y (2010) Graphene based electrochemical sensors and biosensors: a review. Electroanal 22:1027–1036
7. Wang J (2005) Carbon-nanotube based electrochemical biosensors: a review. Electroanal 17:7–14
8. Villalonga R, Díez P, Casado S, Eguílaz M, Yáñez-Sedeño P, Pingarrón JM (2012) Electropolymerized network of polyamidoamine dendron-coated gold nanoparticles as novel nanostructured electrode surface for biosensor construction. Analyst 137:342–348
9. Zhu N, Gao H, Gu Y, Xu Q, He P, Fang Y (2009) PAMAM dendrimer-enhanced DNA biosensors based on electrochemical impedance spectroscopy. Analyst 134:860–866
10. Vögtle F, Richardt G, Werner N (2009) Dendrimer chemistry: concepts, synthesis, properties, applications. Wiley–VCH, Weinheim
11. Endo T, Yoshimura T, Esumi K (2005) Synthesis and catalytic activity of gold–silver binary nanoparticles stabilized by PAMAM dendrimer. J Colloid Interface Sci 286:602–609
12. Crooks RM, Zhao M, Sun L, Chechik V, Yeung LK (2001) Dendrimer-encapsulated metal nanoparticles: synthesis, characterization, and applications to catalysis. Acc Chem Res 34:181–190
13. Xu L, Zhu Y, Tang L, Yang X, Li C (2007) Biosensor based on self-assembling glucose oxidase and dendrimer-encapsulated Pt nanoparticles on carbon nanotubes for glucose detection. Electroanal 19:717–722
14. Zhu Y, Zhu H, Yang X, Xu L, Li C (2007) Sensitive biosensors based on (dendrimer encapsulated Pt nanoparticles)/enzyme multilayers. Electroanal 19:698–703
15. Villalonga R, Cao R, Fragoso A (2007) Supramolecular chemistry of cyclodextrins in enzyme technology. Chem Rev 107:3088–3116
16. Holzinger M, Bouffier L, Villalonga R, Cosnier S (2009) Adamantane/β-cyclodextrin affinity biosensors based on single-walled carbon nanotubes. Biosens Bioelectron 24:1128–1134
17. Villalonga R, Camacho C, Cao R, Hernández J, Matías JC (2007) Amperometric biosensor for xanthine with supramolecular architecture. Chem Commun 942–944
18. Villalonga R, Matos M, Cao R (2007) Construction of an amperometric biosensor for xanthine via supramolecular associations. Electrochem Commun 9:454–458
19. Wang J (2008) Electrochemical glucose biosensors. Chem Rev 108:814–825
20. Cakara D, Kleimann J, Borkovec M (2003) Microscopic protonation equilibria of poly(amidoamine) dendrimers from macroscopic titrations. Macromolecules 36:4201–4207
21. Katsounaros I, Schneider WB, Meier JC, Benedikt U, Biedermann PU, Auer AA, Mayrhofer KJJ (2012) Hydrogen peroxide electrochemistry on platinum: towards understanding the oxygen reduction reaction mechanism. Phys Chem Chem Phys 14:7384–7391
22. Swoboda BEP, Massey V (1965) Purification and properties of glucose oxidase from Aspergillus niger. J Biol Chem 240:2209–2215
23. Wu WC, Huang JL, Tsai YC (2012) Direct electron transfer and biosensing of glucose oxidase immobilized at multiwalled carbon nanotube-alumina-coated silica modified electrode. Mat Sci Eng C 32:983–987
24. Deng C, Chen J, Chen X, Xiao C, Nie L, Yao S (2008) Direct electrochemistry of glucose oxidase and biosensing for glucose based on boron-doped carbon nanotubes modified electrode. Biosens Bioelectron 23:1272–1277
25. Wang Y, Liu L, Li M, Xu S, Gao F (2011) Multifunctional carbon nanotubes for direct electrochemistry of glucose oxidase and glucose bioassay. Biosens Bioelectron 30:107–111
26. Zhang H, Meng Z, Wang Q, Zheng J (2011) A novel glucose biosensor based on direct electrochemistry of glucose oxidase incorporated in biomediated gold nanoparticles–carbon nanotubes composite film. Sens Actuator B Chem 158:23–27
27. Yan XB, Chen XJ, Tay BK, Khor KA (2007) Transparent and flexible glucose biosensor via layer-by-layer assembly of multiwall carbon nanotubes and glucose oxidase. Electrochem Commun 9:1269–1275
28. Li J, Yu J, Zhao F, Zeng B (2007) Direct electrochemistry of glucose oxidase entrapped in nano gold particles-ionic liquid-N, N-dimethylformamide composite film on glassy carbon electrode and glucose sensing. Anal Chim Acta 587:33–40
29. Şenel M, Nergiz C (2012) Novel amperometric glucose biosensor based on covalent immobilization of glucose oxidase on poly (pyrrole propylic acid)/Au nanocomposite. Curr Appl Phys 12:1118–1124
30. Qiu H, Zou F (2012) Fabrication of stratified nanoporous gold for enhanced biosensing. Biosens Bioelectron 35:349–354
31. Male KB, Hrapovic S, Luong JHT (2007) Electrochemically-assisted deposition of oxidases on platinum nanoparticle/multi-walled carbon nanotube-modified electrodes. Analyst 132:1254–1261
32. Qiu C, Wang X, Liu X, Hou S, Ma H (2012) Direct electrochemistry of glucose oxidase immobilized on nanostructured gold thin films and its application to bioelectrochemical glucose sensor. Electrochim Acta 67:140–146
33. Xiao X, Zhou B, Zhu L, Xu L, Tan L, Tang H, Zhang Y, Xie Q, Yao S (2012) An reagentless glucose biosensor based on direct electrochemistry of glucose oxidase immobilized on poly(methylene blue) doped silica nanocomposites. Sens Actuator B Chem 165:126–132